



Structure and properties of composites prepared from partially amorphous ZrCuNiTi and nanocrystalline silver

J. Dutkiewicz*, L. Lityńska-Dobrzyńska, W. Maziarz, T. Czeppe, A. Kukuła, Ł. Rogal

Institute of Metallurgy and Materials Science of the Polish Academy of Sciences, Poland

ARTICLE INFO

Article history:

Received 25 June 2010

Received in revised form 7 February 2011

Accepted 8 February 2011

Available online 12 February 2011

Keywords:

ZrCuNiTi amorphous alloys

Mechanical alloying

Melt spinning

Hot pressing

HRTEM

ABSTRACT

Alloys of composition Zr₄₀Cu₄₀Ni₁₀Ti₁₀ and Zr_{48.5}Cu_{32.5}Ni₉Ti₁₀ (in at.%) were ball milled for 40 h starting from elemental powders or melt spun from cast ingots. In both cases amorphous structure was obtained, however in the case of ribbons, larger crystals of Cu₁₀Zr₇ or Ni₇Zr₂ phases of size of a few hundred nm were observed. In the case of milled alloys much finer intermetallic phases such as Zr₂Cu or Cu₁₀Zr₇ were identified within the amorphous matrix using X-ray diffraction or HRTEM. In both alloys DSC studies have shown higher crystallization temperature for the powder, than for the ribbon. It was explained by a different structure of preexisting intermetallic nuclei crystallizing in milled powders. The milled amorphous powder was also used as a matrix for composites containing 20% or 50% of nanocrystalline silver powder, prepared from silver powder by ball milling. The composites hot pressed at the same temperature as the amorphous samples show in some places very narrow transition phase enriched in silver containing also other elements of the amorphous phase. Composites containing more silver show lower hardness and strength, but exhibit a few percent of plastic deformation in the compression test. Scanning electron studies of deformed composite samples show crack initiation within the amorphous phase, not at the components interfaces.

© 2011 Elsevier B.V. All rights reserved.

1. Introduction

In the quaternary ZrTiCuNi system, the TiCu-rich glass forming region is determined by one or two of the 3 eutectics [1], similarly like for the ZrCu rich region. Multicomponent CuTi base or CuZr base alloys can be easily obtained amorphous by a conventional copper mould casting [2–4] or melt spinning method [5–7]. The alloys from the quaternary CuTiZrNi system show a very good glass forming ability manifested by high values of $T_{rg} = T_g/T_l$ above 0.6 [2,3,5–10]. Cast bulk quaternary CuTiZrNi amorphous alloys show also a very good mechanical properties with a compressive fracture strength above 2 GPa [4–6,11,12], with a positive effect of fine crystalline particles [11]. Among amorphous quaternary and multicomponent alloys some are based on Cu–Ti system [2,3,6–8,11,12] and the other on Cu–Zr system [4,7] either with Ni, Ti or Al additions. Atomized CuTiZrNiSnSi powders were obtained amorphous [12], however sintered already at 470 °C, completely crystallized. On the other hand spark plasma sintered amorphous CuZrNiTi and Ni base atomized powders have shown a very good mechanical properties [13]. The CuZrTiY alloy powder, mechanically alloyed was obtained amorphous with a very high value of

$\Delta T = T_x - T_g$ of 82 °C [14] and the presence of nanoparticles were not affecting this value. Similar observation was reported in ball milled Cu₄₇Ti₃₃Zr₁₁Ni₈Si₁ alloy [10] where crystallization onset of milled powder was 470 °C and that of the hot pressed bulk have shown even higher values.

Therefore in the present paper two compositions of Zr–Cu–Ni–Ti alloy based on Cu–Zr system (less explored than that based on the Cu–Ti system) were chosen to produce amorphous structure either by melt spinning or by ball milling, followed by hot pressing with addition of Ag nanocrystalline powder to produce amorphous-crystalline composite. The crystallization effects were compared in ball milled and melt spun amorphous alloys as the literature results concerning crystallizing phases in quaternary CuZrTiNi alloy system are not consistent [1–12]. The silver addition was chosen to improve ductility and electrical conductivity of composites as in [8,10] which might be useful as electrical contacts materials and to improve glass forming ability [15] in a transition interface regions, where silver is expected to diffuse into amorphous phase.

2. Experimental procedure

Two quaternary alloys were chosen for the present study Zr₄₀Cu₄₀Ti₁₀Ni₁₀ (1) and Zr_{48.5}Cu₃₂Ti₁₀Ni₉ (numbers indicate at.%). The composition of alloy 2 was chosen as that of multicomponent eutectic existing in the as cast alloy 1. Ball milling process of alloys was performed in a planetary mill “Pulverisette 5” at 200 rpm in argon atmosphere using bearing steel balls. High purity elemental powders (≥99.7%) were handled in a glove box under a purified argon atmosphere. The 15 min of

* Corresponding author. Fax: +48 12 6372192.

E-mail address: nmdutkie@imim-pan.krakow.pl (J. Dutkiewicz).

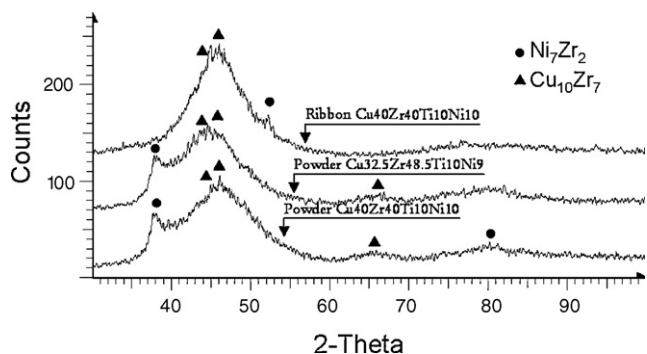


Fig. 1. X-ray diffraction curves from the alloy 1 melt spun ribbon (top), alloy 2 40 h milled powder (middle) and alloy 1 40 h milled powder (bottom).

milling was followed by 45 min of pause for cooling down to avoid overheating of powders. The elemental powders were initially blended to the required compositions and then subjected to ball milling. The identical alloy's compositions were melt spun using equipment built by VACTEC Poland at the copper wheel linear rate of 23 m/s and the ejecting helium gas pressure of 0.15 MPa. Composites were obtained by hot pressing in vacuum of ball milled powder mixtures of amorphous and 20% or 50% of silver powder, previously 40 h ball milled to obtain nanocrystalline structure. Compacting was performed under vacuum of 10^{-2} bar at a pressure of 600 MPa and temperatures several degrees below the crystallization temperature. Thermal effects were studied using Du-Pont Q910 thermal analyser. Mechanical properties were studied using 0.5 MN Instron testing machine using samples of height 6 mm, 4 mm \times 4 mm thick. Structure was studied using HRTEM (Tecna G2F20 S-Twin), Philips XL 30 SEM and X-ray diffractometer PHILIPS PW 1840. Thin foils from composite interfaces for TEM were obtained using FEI FIB instrument, while from powder using Leica EM UC6 ultramicrotome.

3. Results and discussion

3.1. Ball milling or melt spinning amorphization

Fig. 1 shows X-ray diffraction curves for the 40 h milled powder and the melt spun ribbon from the alloy 1 and the milled powder from the alloy 2. One can see that the ribbon shows a broad hallow characteristic for the amorphous phase, while diffraction curves from powders show in spite of the broad hallow, small peaks from

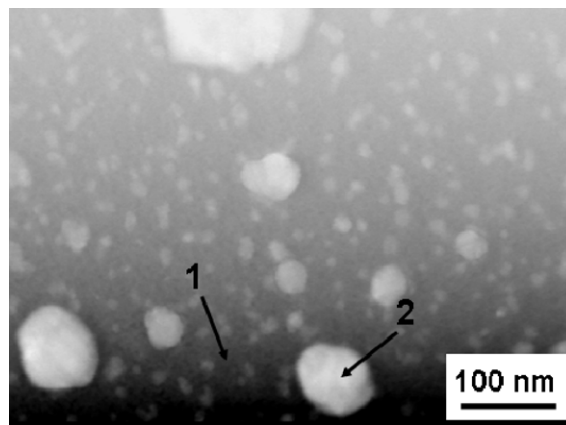


Fig. 3. HAADF micrograph of the melt spun ribbon of the alloy 1 and above the table with the chemical composition measured using EDS detector at points 1 and 2 marked in the micrograph.

the crystalline phase. Due to a small intensity of peaks and probable existence of texture it is difficult to identify crystalline phases, however one can see that position of higher intensity peaks of $Cu_{10}Zr_7$ and Ni_7Zr_2 phases marked on the diffraction curves match fairly well the existing diffraction peaks. These phases were indicated as components of eutectic reactions in the ZrCuNiTi system [1] and $Cu_{10}Zr_7$ was observed in ternary CuZrTi alloys [16]. Fig. 2 shows DSC curves of alloy 2 ball milled or melt spun. A different sequence of crystallization peaks is observed for ribbons and milled powders. One can see that in both cases crystallization occurs in a few stages as manifested by 3 exothermic peaks in the ribbon and 2 in the powder. The maxima for the ribbon are at 464 °C, 563 °C and 613 °C, while for the powder the first strong peak is observed at 519 °C. Similarly for the alloy 1 the first crystallization peak for the powder occurs at 549 °C, while that for the ribbon at 485 °C, confirming observation in Fig. 2 for the alloy 1. Fig. 3 shows a High Angle Annular Dark Field HAADF micrograph of the melt spun ribbon from the alloy 1 and the table as an insert with results of the chemical composition of the amorphous matrix and the bright phase marked as

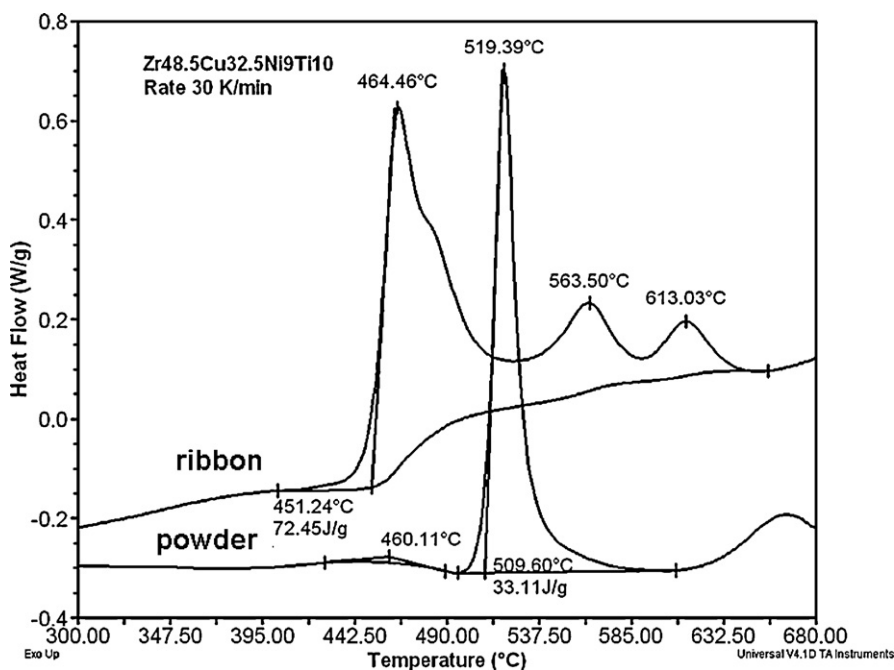


Fig. 2. DSC curves obtained during heating 30 K/min of the alloy 2 powder milled 40 h (bottom) and melt spun ribbon (top).

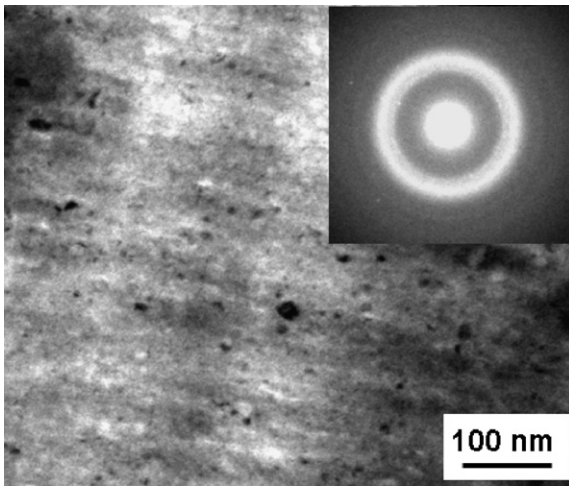


Fig. 4. TEM micrograph of 40 h ball milled alloy 1 and corresponding electron diffraction pattern.

points 1 and 2 in the micrograph. One can see that crystalline particles visible as bright of size from several up to 100 nm are enriched in copper and contain less other elements than the matrix. From the results of the chemical analysis of particles one can expect precipitates from the binary Cu–Zr system and indeed such phases were identified using X-ray diffraction and high resolution transmission electron microscopy. The TEM studies of the structure of the ribbon from the alloy 2 of composition near eutectic [1] have shown much higher fraction of the amorphous phase and only a few small crystalline particles of similar composition as in the alloy 1. Fig. 4 shows a TEM micrograph of a powder particle of 40 h ball milled alloy 1. One can see parallel stripes resulting from multiple ball hitting and welding of individual powder particles and a darker small particles of size 5–20 nm, being most probably intermetallic crystalline phases formed during milling. In the Selected Area Diffraction Pattern (SADP) shown as an insert one can see broad hallow resulting from the amorphous phase and weak diffraction rings from crystals, however there are only few of them and it was not possible to identify existing phases basing on their distance measurements. Fig. 5 shows a High Resolution Transmission Electron Micrograph

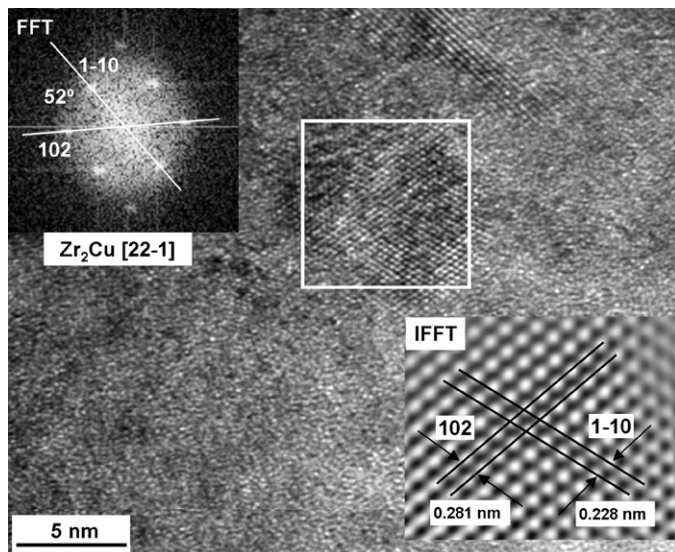


Fig. 5. High Resolution Transmission Electron Micrograph HRTEM from milled powder of the alloy 1, Fast Fourier Transform FFT and Inverse Fast Fourier Transform IFFT from area marked by a square shown as inserts.

HRTEM taken from the 40 h milled powder from the alloy 1. One can see a cross grating of fringes within the area of nanocrystalline inclusion of size of several nanometers. From the distance of fringes and their mutual angles it was found that the crystal can be identified as Zr_2Cu phase in accordance with a tendency of changes of chemical composition within inclusions as shown in Fig. 7. The other HRTEM micrographs allowed to identify the same phase or Cu_2TiZr phase.

3.2. Composites hot pressed from milled powders

The composites were prepared by a short mixing of the milled amorphous powder with either 20 or 50 wt.% of nanocrystalline Ag powder and subsequent hot pressing in vacuum. Fig. 6 shows a scanning electron micrograph of the composites. One can see that both composites show similar microstructures, where amorphous particles are immersed in the silver matrix visible as a bright phase. The amorphous phase is of shape of powder particles after milling. The porosity of the composites is rather small (less than 1%) and the higher silver content allows to decrease the porosity, as the softer silver matrix better fills the die. Fig. 7a shows a HAADF micrograph from the amorphous part of the composite containing 20% of silver and 80% of the amorphous powder from the alloy 1. The composition change along the line 1 marked in the micrograph in Fig. 7a is shown below. Due to the contrast dependence on the Z number in the micrograph one can expect that crystalline inclusions are of different composition, than the amorphous matrix. Indeed, as results from the EDS measurements along the line 1 one can see that a bright particle show an increase of Zr, and decrease of copper content indicating possibility of Zr_2Cu precipitation as in milled powders. However, in other places particles rich in copper and titanium with smaller content of Ni and Zr were also observed. The results obtained using HAADF and EDS techniques indicate that nanocrystalline inclusions possess different composition than that of the amorphous matrix.

Fig. 7b shows a HAADF micrograph of the silver/amorphous interface and below changes of number of X-ray counts in EDS detector indicating changes of chemical composition along the line marked 1 in the micrograph. One can see that in spite of a rather long time of hot pressing, lasting several minutes, there is only an insignificant growth of a transition phases at the interface marked by a bright line in Fig. 7b. This fact might be due to a small solubility of silver in Ti and Ni. The crystalline phases within the amorphous matrix visible in the right side grow similarly to that in ball milled powder, as shown in Fig. 4. There is a gradual decrease of silver and increase of a content of other elements in the transition phase without any preference for one of phases. One can see that the average size of grains within the silver part is in the order of a few hundred of nm, what is the reason of rather high hardness of this part of the composite. The microhardness of the silver matrix is similar in all composites, of the order of 145 HV and Young's modulus about 140 GPa, while the microhardness of the amorphous phase of the alloy 1 in the composites is about 810 HV and the Young's modulus near 185 GPa. The microhardness of the amorphous phase from the alloy 2 is near 1050 HV and the Young's modulus near 160 GPa. The changes of hardness are not however manifested by changes in a compression strength, since they are similar for both composites based on alloys 1 and 2.

Fig. 8a shows a compression curves of the composites based on the alloy 2 with additions of 20 and 50% of Ag. One can see that the compression strength is about 760 MPa for the composite containing 20% Ag and near 600 MPa for the other one. The plastic deformation is slightly higher near 3% and the deformation curve is more smooth for the composite containing 50% Ag, indicating less crack formation and more plastic deformation within the silver part. The compression strength is much lower than reported

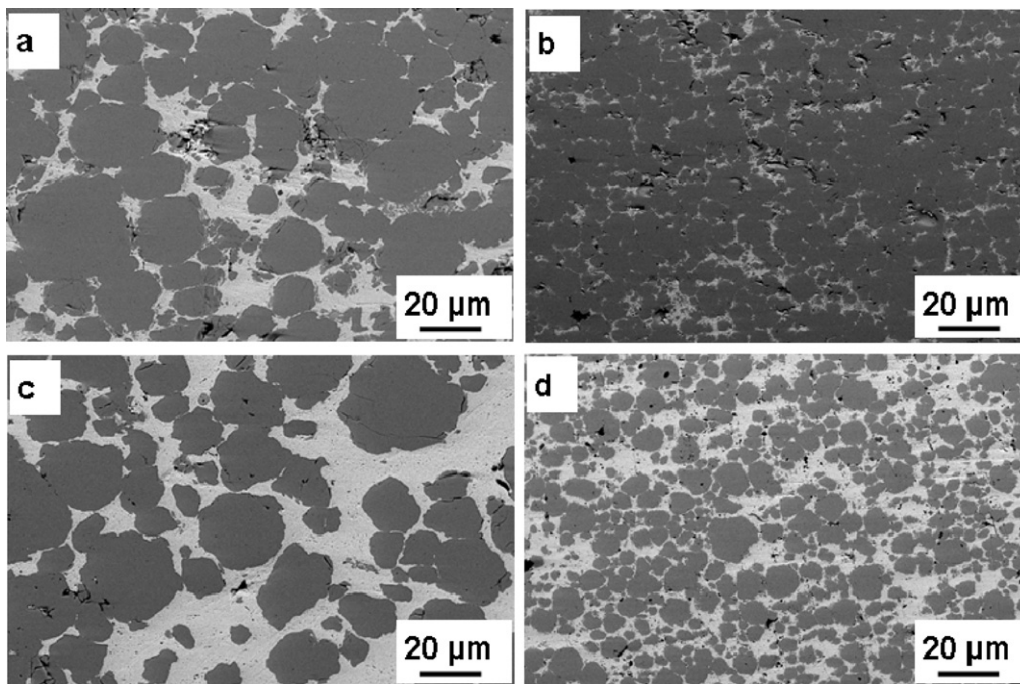


Fig. 6. SEM micrographs of the composites based on alloy 1 (a and c) and alloy 2 (b and d) containing 20% Ag (a and b) and 50% Ag (c and d).

for the cast amorphous alloys [5–7,11,12], however much higher than that for a pure silver. Therefore one can expect that they may be useful for electrical contacts where a high strength and a good conductivity assured by a high content of a pure silver is required.

Fig. 8b shows a SEM micrograph from the composite based of the amorphous powder of the alloy 1 and 50% of silver after a compression test. The microstructures of the deformed composites based on the amorphous alloy 2 are similar. One can see that the crack

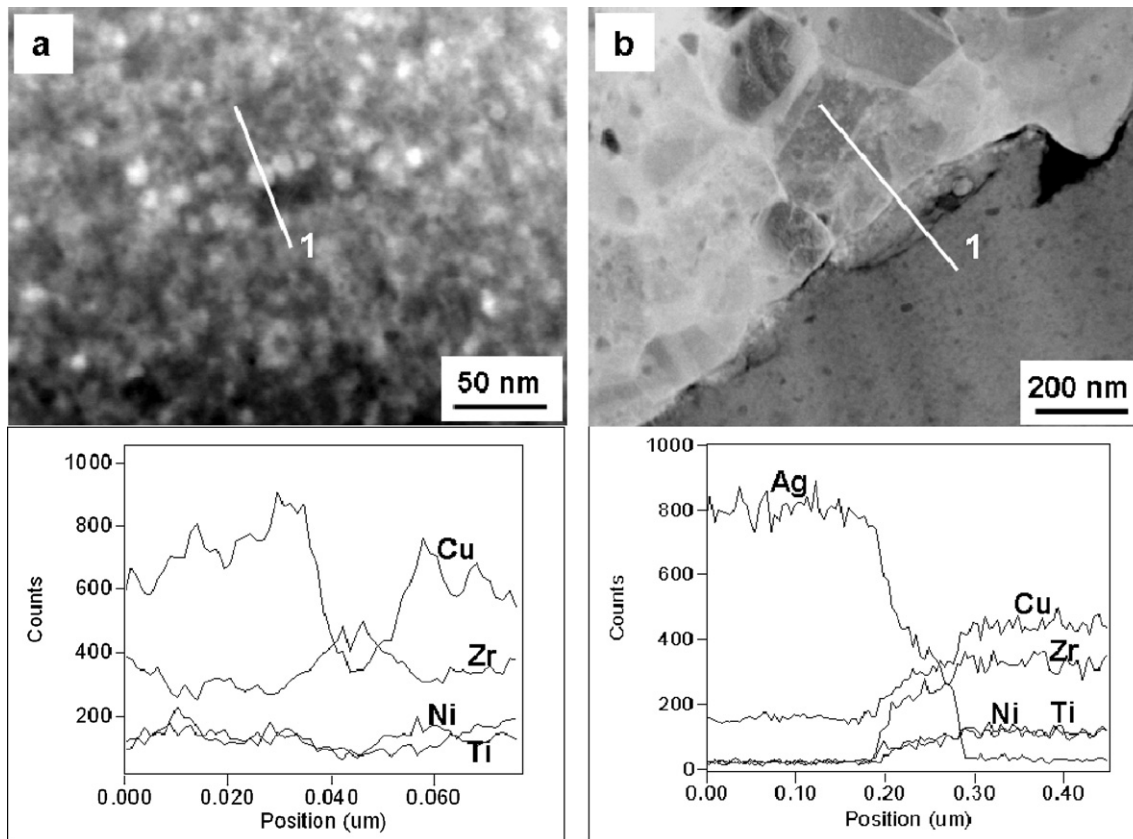


Fig. 7. HAADF micrographs of the composites and below changes of number of X-ray counts in EDS detector indicating changes of chemical composition along the lines 1 marked in the micrographs (a) Alloy 1 containing 20% Ag (b) Alloy 2 with 50% Ag.

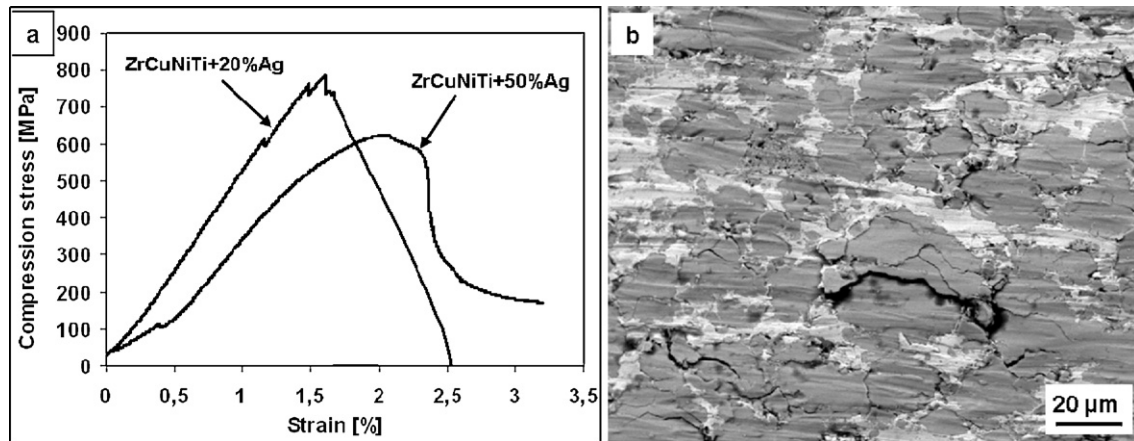


Fig. 8. (a) Compression curves of the composite based on the alloy 2 with 20% Ag and 50% Ag. (b) SEM micrograph of the deformed composite based on the alloy 1 with 50% Ag.

initiation occurs within the amorphous part, not at the interfaces of both components. It indicates that the observed phases formed at the interface visible in Fig. 7b do not cause crack initiation and the amorphous part is responsible for the low plasticity of composites.

4. Conclusions

- Both, ball milling of elemental powders for 40 hours or melt spinning on a rotating copper drum allows to obtain amorphous phase from alloys Zr₄₀Cu₄₀Ni₁₀Ti₁₀ and Zr_{48.5}Cu_{32.5}Ni₉Ti₁₀ (in at.%). The ribbon of the first alloy shows intermetallic particles of size of several nanometers identified as Ni₇Zr₂ or Cu₁₀Zr₇; the same phases, however much of smaller size and volume were found in the second (eutectic) alloy. Ball milled powders contain also intermetallic phases identified as Zr₂Cu and Cu₁₀Zr₇. Different structure of intermetallic phases in ribbons and milled powder might be a reason for the about 50 °C higher crystallization temperatures in the milled amorphous powders in both investigated alloys.
- The composites prepared by mixing of milled amorphous powders and the nanocrystalline silver powder in proportions of 20 and 50 wt.%, hot pressed in vacuum at a temperatures below T_x have shown a low porosity below 1%. The microhardness of the amorphous phase was about 800–1000 HV, while that of silver 140–160 HV. The compression strength of a composite containing 20% Ag was near 750 MPa, while at 50% of silver about 600 MPa. Both composites have shown about 1% of the elastic deformation and about 3% of the plastic strain.

Acknowledgements

Financial support from the Research Grant from the Ministry of Science and Higher Education Nr NN507348035 is gratefully acknowledged.

References

- [1] D. Ma, H. Cao, Y.A. Chang, *Intermetallics* 15 (2007) 1122.
- [2] Y.J. Yang, D.W. Xing, C.P. Li, S.D. Wei, J.K. Sun, Q.K. Shen, *Mater. Sci. Eng. A* 448 (2007) 15.
- [3] X.F. Wu, Z.Y. Suo, Y. Si, L.K. Meng, K.Q. Qiu, *J. Alloys Compd.* 452 (2008) 268.
- [4] J. Eckert, J. Das, K.B. Kim, F. Baier, M.B. Tang, W.H. Wang, Z.F. Zhang, *Intermetallics* 14 (2006), 876 M.
- [5] J. Eckert Seidel, L. Schultz, *Mater. Lett.* 23 (1995) 299.
- [6] J. Wang, B. Liu, L. Wang, Y. Wu, L. Wang, *J. Non-Cryst. Solids* 354 (2008) 3653.
- [7] X.H. Lin, W.L. Johnson, *J. Appl. Phys.* 78 (1995) 6514.
- [8] J. Dutkiewicz, J. Morgiel, L. Lityńska-Dobrzyńska, W. Maziarz, T. Czeppe, M. Carillo-Parra, T.B. Massalski, *Arch. Metall. Mater.* 51 (2006) 525.
- [9] Y.J. Yang, Q.J. Chen, S.S. Shan, H.W. Liu, L.M. Qiao, C.X. Liu, *J. Alloys Compd.* 480 (2009) 329.
- [10] J. Dutkiewicz, L. Lityńska-Dobrzyńska, Ł. Rogal, W. Maziarz, T. Czeppe, *Phys. Stat. Sol. A* 207 (2010) 1109.
- [11] M. Calin 1, J. Eckert, L. Schultz, *Scripta Mater.* 48 (2003) 653.
- [12] C.K. Kim, C.-Y. Son, D.J. Ha, T.S. Yoon, S. Lee, N.J. Kim, *Mater. Sci. Eng. A* 476 (2008) 69.
- [13] T.-S. Kim, J.-Y. Ryu, J.-K. Lee, J.-C. Bae, *Mater. Sci. Eng. A* 449–451 (2007) 804.
- [14] P.-Y. Lee, C.-J. Yao, J.-S. Chen, L.-Y. Wang, R.-R. Jeng, Y.-L. Lin, *Mater. Sci. Eng. A* 375–377 (2004) 829.
- [15] E.S. Park, H.J. Chang, D.H. Kim, T. Ohkubo, K. Hono, *Scripta Mater.* 54 (2006) 1569.
- [16] U.E. Klotz, C. Liu, P.J. Uggowitzer, J.F. Löffler, *Intermetallics* 15 (2007) 1666.